Diversity and Distributions A Journal of Conservation Biogeography

Spatial patterns of seagrass dispersal and settlement

Journal:	*Diversity and Distributions*
Manuscript ID	DDI-2016-0073.R1
Manuscript Type:	Biodiversity Research
Date Submitted by the Author:	n/a
Complete List of Authors:	Grech, Alana; Macquarie University, Department of Environmental Sciences Wolter, Jolan; Universite Catholique de Louvain, Earth and Life Institute (ELI) Coles, Rob; James Cook University, Centre for Tropical Water & Aquatic Ecosystem Research McKenzie, Len; James Cook University, Centre for Tropical Water & Aquatic Ecosystem Research Rasheed, Michael; James Cook University, Centre for Tropical Water & Aquatic Ecosystem Research Thomas, Christopher; Université catholique de Louvain, Institute of Mechanics, Materials and Civil Engineering (iMMC) Waycott, Michelle; University of Adelaide, School of Biological Sciences, Environment Institute, Australian Centre for Evolutionary Biology and Biodiversity Hanert, Emmanuel; Université catholique de Louvain, Earth and Life Institute (ELI)
Keywords:	dispersal, Great Barrier Reef, hydrodynamics, seagrass, recovery, resilience

Note: The following files were submitted by the author for peer review, but cannot be converted to PDF. You must view these files (e.g. movies) online.

0801N3_sub.mp4
0801N3_sur.mp4
0801N16_sub.mp4
0801N16_sur.mp4
0801N24_sub.mp4
0801N24_sur.mp4
0801N29_sub.mp4
0801N29_sur.mp4
0903N3_sub.mp4
0903N3_sur.mp4
0903N16_sub.mp4
0903N16_sur.mp4
0903N24_sub.mp4
0903N24_sur.mp4
0903N29_sub.mp4

0903N29_sur.mp4
1001N3_sub.mp4
1001N3_sur.mp4
1001N16_sub.mp4
1001N16_sur.mp4
1001N24_sub.mp4
1001N24_sur.mp4
1001N29_sub.mp4
1001N29_sur.mp4
1102N3_sub.mp4
1102N3_sur.mp4
1102N16_sub.mp4
1102N16_sur.mp4
1102N24_sub.mp4
1102N24_sur.mp4
1102N29_sub.mp4
1102N29_sur.mp4

Title: Spatial patterns of seagrass dispersal and settlement

Running head: Spatial patterns of seagrass dispersal

Authors: Alana Grech[1]*, Jolan Wolter[2]*, Rob Coles[3], Len McKenzie[3], Michael Rasheed[3], Christopher Thomas[4], Michelle Waycott[5], Emmanuel Hanert[2]

[1] Department of Environmental Sciences, Macquarie University, Sydney, New South Wales, Australia, 2109

[2] Earth and Life Institute (ELI), Université catholique de Louvain, Louvain-la-Neuve, Belgium, 1348

[3] TropWATER (Centre for Tropical Water & Aquatic Ecosystem Research), James Cook University, Cairns, Queensland, Australia, 4870

[4] Institute of Mechanics, Materials and Civil Engineering, Université catholique de Louvain, Louvain-la-Neuve, Belgium, 1348

[5] School of Biological Sciences, Environment Institute, Australian Centre for Evolutionary Biology and Biodiversity, The University of Adelaide, South Australia, Australia, 5001

*These authors contributed equally to this manuscript

Corresponding author:

Dr Alana Grech

Department of Environmental Sciences, Macquarie University

Sydney, New South Wales, 2109, Australia

Email: Alana.grech@mq.edu.au Telephone: +61 2 9850 7477

Word count: 5016

Abstract

Aim The movement of propagules among plant populations affects their ability to replenish and recover after a disturbance. Quantitative data on recovery strategies, including the effectiveness of population connectivity, is often lacking at broad spatial and temporal scales. We use numerical modelling to predict seagrass propagule dispersal and settlement to provide an approach for circumstances where direct, or even indirect, measures of population dynamics are difficult to establish.

Location Great Barrier Reef, Australia

Methods We used the finite element *Second-generation Louvain-la-Neuve Ice-ocean Model* (SLIM) to resolve the hydrodynamics of the central Great Barrier Reef and to simulate the dispersal of seagrass. We predicted dispersal and settlement patterns by releasing 10.6 million passive particles representing seagrass propagules at known sites of seagrass presence. We considered two fractions when modelling seagrass dispersal: floating and suspended propagules. Both fractions were modelled using 34 simulations run for a maximum of 8 weeks during the peak seagrass reproductive period, capturing variability in winds, tides and currents.

Results The ‘virtual’ seagrass propagules moved on average between 30 and 60 km, but distances of over 900 km also occurred. Most particle movement was to the north-west. The season (month) of release and source locations of the particles correlated with their dispersal distance, particularly for particles released offshore, with the complex coastal topography impeding movements close to the coast. The replenishment and recovery potential of the northern most meadows was influenced by southern meadows. Protected north facing bays were less likely to receive particles.

Main conclusions Our approach advances the conservation and management of marine biodiversity by predicting a key component of ecosystem resilience at a spatial scale that informs marine planning. We show a complex interaction among time, wind, water movement and topography that can guide a management response to improving replenishment and recovery after disturbance events.

Key words: Dispersal, Great Barrier Reef, hydrodynamics, seagrass, recovery, resilience

(A) Introduction

Safeguarding biodiversity and the delivery of marine ecosystem services requires the maintenance of ecological processes that underpin their functioning and resilience (Roberts *et al.* 2003; Magris *et al.* 2014). The multiple factors that contribute to resilience and their interactions are complex (Kilminster *et al.* 2015; Unsworth *et al.* 2015). An important component of marine ecosystem resilience is the capacity to recover from loss or degradation. Recovery is supported by the dispersal of larvae, adults or propagules via the convective forces of ocean waves and currents (Berumen *et al.* 2012; Bode *et al.* 2012). The rate of exchange or connectivity among populations effects the replenishment and recovery of populations after major disturbances (e.g. storms) and population dynamics (Treml *et al.* 2008). However, our understanding of dispersal and connectivity via ocean waves and currents is poor for many ecosystems, especially seagrasses (McMahon *et al.* 2014).

Seagrasses comprise a group of angiosperms that have successfully dispersed and colonised throughout the world's coastal seabeds. Seagrass meadows can be found on all continents except Antarctica, and from the high intertidal zone down to 61 m deep (Coles *et al.* 2009). The 15 species that are found in the Great Barrier Reef World Heritage Area (GBR) in north eastern Australia (Fig. 1) are a vital part of the reef ecosystem and provide food for numerous fish, crustacean, sea turtles and dugong (Unsworth *et al.* 2014). Seagrasses are widespread in these waters (Coles *et al.* 2009; Grech and Coles 2010), however recent tropical cyclones and floods have had severe impacts on the viability of some meadows and resulted in losses occurring at scales of hundreds of kilometres (Rasheed *et al.* 2014; Coles *et al.* 2015; McKenna *et al.* 2015).

The effect of climatic disturbances on seagrasses in the GBR is exacerbated by the impacts of coastal development and poor water quality (Coles *et al.* 2015). Predicting the effect of disturbances and potential recovery trajectories requires information on factors influencing resilience of seagrass meadows, including replenishment and recolonization modes (Kendrick *et al.* 2012).

Propagule dispersal has been well studied in terrestrial plants, although the predictability of successful dispersal mechanisms is less well understood, particularly over longer distances and when animal mediated (Nathan *et al.* 2008; Nathan and Muller-Landau 2000). Propagules can be seeds, fruit or viable plant fragments. Dispersal mechanisms include movement with wind, waterborne, through ingestion by or attachment onto birds and land animals, and through various transport methods during the movement of soil. Seed pollination can be mediated by insects or wind transport. Wholly marine seagrass species can grow and colonise vegetatively by rhizome extension over short distances (100s of metres), but must use other mechanisms for dispersal over broad spatial scales. Most seagrass fruits are short-lived, and have negatively buoyant seeds with primary movement likely to be no more than several kilometres (Kendrick *et al.* 2012; Berković *et al.* 2014). Seagrass seeds can also be transported in the gut and faeces of fish, water fowl, sea turtles and dugongs (McMahon 2005; Sumoski and Orth 2012; Tulipani and Lipcius 2014); viable seeds have been found in the faeces of dugong (James Cook University, unpublished data). However, for tropical and sub-tropical seagrass species, by far the most likely mechanism for transport over broad spatial scales is by waterborne transport of viable propagules (i.e. vegetative fragments, fruits and plant fragments with attached fruits and seeds) (Berković *et al.* 2014). Buoyancy and survival times (although not necessarily leading to successful establishment) for seagrass propagules may be as long as 85 days in temperate species (Thomson *et al.* 2014), but varies for subtropical species with 0.5 days for *H. decipiens*, 4.5 days for *H. ovalis* and 21 days for *Z. muelleri* (Weatherall *et al.* 2016). The maximum dispersal distances recorded in literature are generally less than 100 km, except during extreme weather events when dispersal has been recorded over distances of up to 400 km (Lacap *et al.* 2002).

There is a considerable body of literature on survival of propagules in the water column, as well as on their buoyancy and potential distance moved (Ruiz-Montoya *et al.* 2012; McMahon *et al.* 2014). However, there is little comprehensive analysis using hydrodynamics to predict seagrass dispersal over broad scales (Ruiz-Montoya *et al.* 2012 e.g. Erftemeijer *et al.* 2008; Källström *et al.* 2008; Ruiz-Montoya *et al.* 2015), and no studies relevant to tropical species. This leaves a gap in our ability to provide management agencies with evidence-based science on the capacity for the replenishment and recovery of tropical seagrass meadows from natural and anthropogenic disturbances.

The focus of this study was to address this gap using as an example the spatial dispersal of seagrass propagules in the central GBR, an area encompassing the major regional city and port of Townsville, as well as Hinchinbrook Island, Cleveland Bay, Bowling Green Bay and the Whitsunday Islands (Fig. 1). It is one of a few regions in the world with a long history of seagrass research and mapping (Coles *et al.* 2007; McKenzie *et al.* 2010; Petus *et al.* 2014) as seagrasses in the area are exposed to urban and port developments, poor water quality from terrestrial runoff and tropical storms (Grech *et al.* 2011; Rasheed *et al.* 2014; Coles *et al.* 2015).

Effective management is therefore required to protect and enhance seagrass resilience and its subsequent long-term survival.

We used a numerical modelling approach to resolve the hydrodynamics of the central GBR and to simulate the dispersal of floating and suspended 'virtual' seagrass propagules. The hydrodynamic model used was the finite element *Second-generation Louvain-la-Neuve Ice-ocean Model* (SLIM), a model ideally suited to studying areas of complex topography and flow patterns at very high spatial resolution (Lambrechts *et al.* 2008). We predicted the dispersal and settlement patterns of seagrass by simulating the release of millions of passive 'virtual' propagules (seagrass propagules are represented as particles in the model) at known sites of seagrass presence. The simulations were timed to capture variability in winds, currents, and tides during the peak seagrass reproductive period. The simulation outputs were used to identify factors which facilitate abiotic seagrass dispersal and settlement, and to assess, spatially, the likelihood of replenishment and post-disturbance recovery of seagrass meadows in the central GBR.

(A) Methods

(B) Study region

The central GBR coast between 17.5°S and 20.7°S (~730 km) is characterised by a series of small estuaries and north-facing bays (Fig. 1A). The region includes the city and port of Townsville, and a developing port at Abbot Point near the town of Bowen. The largest island in the GBR, Hinchinbrook, is in the north, and the complex of islands that make up the tourist destination of the Whitsunday Islands is in the south. The climate is influenced by monsoonal wind and rainfall patterns. Strong south-easterly winds dominate during the dry season (April–October). Weaker variable winds are more common during the wet (monsoon) season (November–March).

Water circulation on the GBR continental shelf is driven by tides, wind and water exchanges with the neighbouring Coral Sea (Wolanski *et al.* 2013). Tides in the GBR range from 2.5 – 9 m (Hopley *et al.* 2007) and tidal currents play an important role in cross-shelf mixing, though their amplitude can vary considerably with latitude (Andrews and Bode 1988). The westward-flowing South Equatorial Current impinges on the GBR continental shelf from the Coral Sea, bifurcates into northward and southward components, and drives the southward-flowing Coral Sea Lagoonal Current through the central and southern parts of the GBR, and the East Australian Current at the shelf break and seaward of it (Church and Boland 1983; Church 1987; Wolanski *et al.* 2013). During periods of sustained south-easterly trade winds however, these act to drive a northward longshore current through the central and southern regions of the GBR which opposes the Coral Sea Lagoonal Current, and can result in a reversal of the net direction of flow through the shelf, towards the north (Andrews and Furnas 1986). At finer scales, flow patterns are influenced by the high complexity of the reef topography (Wolanski and Spagnol 2001; Hamann *et al.* 2011; Thomas *et al.* 2014).

(B) Seagrass distribution

We investigated the dispersal of the most common seagrass genera in the central GBR: *Halophila*, *Halodule, Cymodocea* and *Zostera* (Lee Long *et al.* 1993; Carruthers *et al.* 2002; Coles *et al.* 2003). A spatial (geographic information system [GIS]) layer of intertidal and shallow subtidal seagrass distribution was obtained from McKenzie *et al.* (2014a) (Fig. 1A and 2). The layer incorporates the composite outputs of seagrass surveys conducted between November 1984 and June 2010 (McKenzie *et al.* 2010). The total area of intertidal and shallow subtidal seagrass in the study region was 848.3 km^2, and the number of meadows 121. The size of individual meadows ranged from 0.4 – 155.0 km^2 (mean = 7.0 km^2; *see* Table S1 in Supporting Information).

Each intertidal and shallow subtidal meadow was allocated into one of two generalised species classes to facilitate analysis of dispersal and settlement among meadows dominated by species of similar life-history traits (Fig. 1A and 2) (*see* Kilminster *et al.* 2015 for full discussion): the structurally robust opportunistic and persistent tropical seagrass species (genera *Halodule, Cymodocea* and *Zostera*) (n = 83), hereafter referred to as foundation species; and the structurally small ephemeral and transient species of the genus *Halophila* (n = 41), hereafter referred to as non-foundation species. We also allocated meadows into 28 discrete habitat units (Fig. 2) based on their species class and similarities in biogeographic properties (i.e. located in the same bay, estuary or island system) to facilitate statistical analysis (Table S1).

A spatial layer of deep-water (> 15 metres depth) seagrass (genus *Halophila*; non-foundation species) was obtained from Coles *et al.* (2009). We assumed that *Halophila* was present at locations where the layer predicted a > 25 % likelihood of seagrass presence. The total area of deep-water seagrass with a > 25 % likelihood of seagrass presence in the study area was 5,792.5 km^2. We divided the deep-water layer into three meadows and discrete habitat units (Fig. 2) of approximately equal latitudinal distance to facilitate statistical analysis (Table S1).

(B) Oceanographic model

The dispersal of 'virtual' seagrass propagules (i.e. fruit, seeds or fruit attached to plant material or viable fragments) was modelled using the finite element, unstructured-grid ocean model SLIM (Legrand *et al*. 2006; Lambrechts *et al.* 2008) in Gmsh (Geuzaine and Remacle, 2009). SLIM is well suited to modelling complex oceanography because of its variable resolution; the model has a fine scale spatial resolution near the coast, reefs and islands (minimum 200 m), and coarser resolution in homogenous areas (maximum 5 km). SLIM has previously been calibrated and used to simulate the hydrodynamics and sediment transport in the GBR (Lambrechts *et al.* 2008; Andutta *et al.* 2012), as well as dispersal of coral larvae (Thomas *et al.* 2014 and 2015) and turtle hatchlings (Hamann *et al.* 2011).

Data on daily wind speed and direction (9 am and 3 pm) and tides for the time period August 1st 2012 – January 31st 2013 were obtained from the Australian Bureau of Meteorology, NOAA NCDC Climate Forecast System Reanalysis (Saha *et al.* 2014) and the TOPEX satellite altimetry (Egbert and Erofeeva 2002). Depth-integrated shallow-water equations were used to compute the water elevation η and the current 2D velocity vector $\boldsymbol{u}$:

(1) $$\frac{\partial \eta}{\partial t} + \boldsymbol{\nabla} \cdot (H\boldsymbol{u}) = 0$$

$$\frac{\partial \boldsymbol{u}}{\partial t} + (\boldsymbol{u} \cdot \boldsymbol{\nabla})\boldsymbol{u} = -f\boldsymbol{e}_z \times \boldsymbol{u} - g\boldsymbol{\nabla}\eta - C_D|\boldsymbol{u}|\boldsymbol{u} + \frac{\boldsymbol{\tau}}{\rho H} + \frac{1}{H}\boldsymbol{\nabla} \cdot [H\nu(\boldsymbol{\nabla}\boldsymbol{u})] \tag{2}$$

where H is the water column depth, f is the Coriolis factor, $\boldsymbol{e}_z$ is a unit vector pointing vertically upwards, g is the gravitational acceleration, C_D is the bottom stress coefficient, $\boldsymbol{\tau}$ is the surface wind stress, ρ is the water density and ν is the horizontal eddy viscosity. The model parameters and external forcing were taken from Thomas *et al.* (2014).

The dispersal of passive 'virtual' propagules (i.e. particles were unable to direct their own motion) was simulated using a Lagrangian Particle Tracker, similar to Spagnol *et al.* (2002). This model uses a random walk formulation of the 2D advection-diffusion equation:

$$\boldsymbol{x}_{n+1} = \boldsymbol{x}_n + \boldsymbol{v}_n \Delta t + \frac{\boldsymbol{R}_n}{\sqrt{r}}\sqrt{2K\Delta t} \tag{3}$$

$$\boldsymbol{v}_n = \left(\boldsymbol{u} + C_w \boldsymbol{u}_w + \frac{K}{H}\boldsymbol{\nabla}H + \boldsymbol{\nabla}K\right)\Big|_{\boldsymbol{x}_n} \tag{4}$$

where $\boldsymbol{x}_n$ and $\boldsymbol{x}_{n+1}$ are the particle positions at iterations n and $n+1$, Δt is the time interval between iterations, $\boldsymbol{R}_n$ is a horizontal vector of zero-mean random numbers of variance r, $\boldsymbol{u}$ the depth-averaged horizontal water velocity computed from Eq. (2), $\boldsymbol{u}_w$ is the wind velocity at a height of 10 m over the sea surface, C_w is the wind drag coefficient and K is the horizontal diffusivity coefficient.

(B) Simulation parameters

The time period of simulations covered the southern hemisphere spring reproductive period (Table 1), which follows the peak of the flowering period and time of highest seagrass abundance (beginning of August through to the end of November; Waycott *et al.* 2004; Kuo *et al.* 1991 and 1993; Kuo and Kirkman 1992). The start dates of individual simulations were chosen to capture variability in tides (spring, neap, and first and last quarter tides) across the reproductive period (Table 1).

The total number of particles (representing 'virtual' seagrass propagules) released per simulation was optimised for the model domain (n = ~154,000). An equal number of particles were released per release location. Release locations were spread evenly across intertidal and shallow subtidal meadow at intervals of ~2 km (n = 266; Fig. 1B). Meadows of size < 4 km^2 had one release location placed at its geometric centre. Release locations were spread evenly across each deep-water meadow at intervals of ~10 km (n = 53). The number of particles released per unit area was smaller in deep-water meadows than in intertidal and shallow subtidal meadows because deep-water seagrasses generally have lower biomass and abundance relative to coastal seagrass (Coles *et al.* 2007; Coles *et al.* 2009; Rasheed *et al.* 2014). Particles were released at an equal rate over the first 24 hours of the simulations to capture daily variation in tidal conditions.

We assumed that the size and shape of seagrass propagules (fruit, seeds or fruit attached to plant material or viable fragments) were the same. We attempted to capture variability in the buoyancy of 'virtual' propagules by simulating the dispersal of propagules floating at the surface and suspended below the surface, and by using a first-order decay function to simulate the gradual settlement of propagules, as described below.

We considered two different fractions when modelling seagrass dispersal using our 'virtual' propagules: (1) floating propagules; and (2) suspended propagules. In Eq. (4), the term depending on the wind velocity represents the wind contribution to the particle advecting velocity. The value of the wind drag coefficient C_w is usually determined empirically as it depends on the particle mass, shape, buoyancy and the wind angle of attack. We used a sensitivity analysis to determine the wind drag coefficient by running 8 simulations with C_w = 0.5, 1, 1.5, 2, 2.5, 3, 3.5 and 4 % and measured the distance between release and settling location. Increasing the wind drag coefficient resulted in particles moving further from their release location in a linear function. We used the outputs of the sensitivity analysis to determine a conservative wind drag coefficient of 2 % (i.e. a velocity equal to 2 % of the wind speed was added to the velocity of the particles) when 'virtual' propagules were assumed to float at the surface. Erftemeijer *et al.* (2008) and Harwell and Orth (2002) use a wind drag coefficient of 3 % to predict the dispersal of the structurally more robust northern hemisphere *Zostera marina* (eelgrass) fragments with reproductive shoots that contain seeds. However, the fragments and seeds of eelgrass are much larger then tropical seagrass propagules. A wind drag coefficient of 0 % was used when particles were suspended below the surface.

Two sets of simulations were conducted at each start date with either 2% and 0% wind drag coefficients to assess differences in the dispersal of floating and suspended particles, and the role of wind in particle transport (n = 68). The ratio of floating and suspended propagule fractions in the central GBR at any given time is unknown. We assumed that the outputs of the two sets of simulations represent equally plausible realities based on our present knowledge.

Each of the 68 simulations were run for a maximum likely survival time of propagules in the tropics (8 weeks/56 days; Lacap *et al.* 2002; Harwell and Orth 2002; Hall *et al.* 2006; Källström *et al.*, 2008, Kendrick *et al.* 2012; Thompson *et al.* 2014). A first-order decay function was used to simulate the gradual settlement of particles after their release following a previously published approach (Erftemeijer *et al.* 2008; Fig. S1):

(5) $C(t) = C_0 \cdot e^{-kt}$

where the decay rate $k = 0.075$ day^{-1} (Erftemeijer *et al.* 2008) and $C(t)$ is the particle concentration at time t.

(B) Statistical analysis and replenishment index

Dispersal distance was calculated as the Euclidean distance between the release location and the settling location in ArcGIS® 10.3. The dispersal distance was aggregated at each release location for the 34 simulations of floating propagules and the 34 simulations of suspended propagules, and the 95th percentile calculated. We used a linear mixed-effect model (package 'nlme') in R (R Core Team 2013) and release location as a random factor to test for significant effects of predictor variables on the dispersal distance of particles at each release location: month of release (August, September, October or November); tide on start date of simulation (neap, spring or first and last quarter tide); depth (intertidal/subtidal or deep); species (foundation or non-foundation species); and Euclidean distance (metres) between mainland coast and release location. The continuous variables of dispersal distance and distance to coast were log transformed to achieve normal distribution and heterogeneity of variances. Model selection was conducted using the function ‘dredge' in R package ‘MuMIn'. The model with lowest AICc value was considered as ‘best fit’. Competing models were ignored because deltaAIC values were > 3 and virtually all weight was given to the first model.

The study region was converted to a raster grid of 1 km^2 resolution. We calculated the number of settled particles and the number of discrete habitat units that were sources of the settled particles at each 1 km^2 grid cell. We assumed that the capacity of a meadow to recover from a disturbance depends on both the number of particles that settle on that meadow and on the number of different sources from which these particles originate. We used discrete habitat units rather than meadows as an indicator of the number of source locations due to the large variability in size and number of individual meadows in the region (Table S1). A potential replenishment index was mapped for both foundation and non-foundation species classes by multiplying the logarithm of the number of settled particles by the number of source discrete habitat units at each grid cell. We used the logarithm of the number of particles for visualisation purposes.

(A) Results

Our simulations predicted a mean dispersal distance of floating ‘virtual’ seagrass propagules (particles) of 60.0 km, and suspended particles of 33.8 km. The maximum dispersal distance of particles was 950 km (simulation of floating particles, release 1 August, discrete habitat unit 31) and a minimum distance of 0 km (simulations of suspended particles, 29 August, 7 October, 17

October, 25 November, discrete habitat units 22 and 19). Animations of seagrass dispersal simulations at multiple locations and release dates are provided in Appendix S1.

Boxplots (Fig. 3) summarise the range of possible dispersal distances of particles for each discrete habitat unit (Fig. 2) generated by the 34 simulations of floating particles and 34 simulations of suspended particles. Simulations of floating particles were affected by wind and had higher dispersal distances (i.e. particles moved further) than simulations that were not affected by wind (i.e. suspended particles). The deep-water non-foundation meadows (discrete habitat units 29, 30 and 31) had the highest range and median dispersal distances for both floating and suspended particles. Particles released from deep-water meadows and coastal regions of high exposure to wind activity (e.g. discrete habitat units 7, 8, 28, 4, 2; Fig. 2) travelled further than meadows in protected bays because they were exposed to strong offshore currents or were not trapped by tidal movements in complex coastal topographic features (Fig. 3).

We used the orientation of settlement locations relative to release locations to develop wind roses of the proportion of floating and suspended particles dispersed at various directions and distances (Fig. 4). Most (77%) floating particles were dispersed towards the north-west quadrant because the seagrass reproductive period is dominated by south-easterly trade winds. Most suspended particles were also dispersed towards the north-west quadrant due to wind-induced water currents, however 32% of particles were dispersed towards the south-east quadrant due to strong water current movement in that direction in September.

Particles released from the southern limit of our modelling domain (i.e. discrete habitat unit 9; Fig. 2) did not move towards the north-west and were either trapped in Repulse Bay, or were moved south-eastwards by water currents. Particles released from the adjacent Whitsunday Islands moved towards the north-west and settled in deep offshore waters and some coastal locations. Due to the shape and direction of the coast south of Repulse Bay (Fig. 1C), it is likely that the southern limit of seagrass connectivity in the central GBR is the Whitsunday Islands.

The linear mixed-effect models of floating and suspended particles at the 95^{th} percentile (Table S2) showed significant seasonal effects (month), and species (foundation and non-foundation) and location (distance to coast) effects. The south-east trade winds, a feature of the region during the mid-year winter, decrease towards the beginning of the monsoon in summer, influencing propagule movement through direct wind effects and indirectly through movement of water. Particles from meadow locations away from the coast in deeper water travelled further than those from coastal locations (Fig. 3) as they entered ocean currents and winds unimpeded by the configuration of coastal topography. Deeper meadows are also populated by non-foundation species and not the foundation species, leading to significant interaction terms.

The potential replenishment indexes of both foundation and non-foundation species indicate a site's relative potential for re-establishment and recovery of seagrass via natural biotic processes (Fig. 5). High levels of replenishment potential were observed along most of the coast. Coastal areas of low replenishment potential included the southern edge of protected bays (e.g. Cleveland Bay, Bowling Green Bay, Upstart Bay), and Edgecombe Bay, Repulse Bay and the Whitsunday Islands. The shape of Edgecombe Bay shelters most of the bay from south-easterly winds, preventing seagrass propagules from neighbouring southern meadows from entering the site. The Whitsunday Islands are exposed to strong south-easterly winds and seagrass propagules are quickly transported away from their release locations. The region between Townsville and Hinchinbrook Island also had a low level of replenishment potential for foundation species, but a higher level of replenishment potential for non-foundation species because of settlement of propagules from deep-water seagrass meadows.

(A) Discussion

We used hydrodynamic modelling and parameters informed by literature to investigate the potential dispersal and settlement patterns of simulated particles representing seagrass propagules in the central GBR. This approach enabled the assessment of factors that influence an important component of resilience: the potential for re-establishment of seagrass meadows after loss or damage (Unsworth *et al.* 2015). From a global perspective, the knowledge gaps identified in this process are first in the assumptions that viable propagules do actually settle and establish as plants in a new location, and that the physical characteristics of propagule fragments of different species interact with wind and water movements in the same way; and second in our poor overall understanding of the movement behaviour of propagules (including loss rates and buoyancy times) in the real world of open ocean transport. The size and density of seeds, fruits and vegetative fragments can vary over orders of magnitude (mms to 10 cms; Oldham et al. 2014) and more information is needed to appropriately incorporate this variation in hydrodynamic models. Our results based on the example of the central GBR represent a theoretical approach to modelling seagrass dispersal based on the best available knowledge to provide an insight into how these complex systems work at a scale that is useful for management. Our results also enable testing of hypotheses to evaluate the specifics of dispersal ranges by testing this model *in situ*.

The results of the simulations indicated that most seagrass propagules on average do not travel far from their source location, especially when suspended in the water column. The average distance travelled by particles within the 8 week time period was between 30 and 60 km (Fig. 3). Particles from deep-water meadows travelled further than those closer to the coast (Fig. 3). 77 % of particles had a northerly component to movement if floating and slightly less when suspended (Fig. 4). Time of release influenced the distance travelled with longer distances observed earlier in the reproductive period due to the greater strength of south-easterly trade winds in August and September compared with later in the year.

Coastal topography influenced the trajectory of particles in the model. Model release locations in offshore meadows allowed particles to move unimpeded and travel further than coastal meadows. Topography also influenced the number of discrete habitat units that could contribute to a recipient meadow (a likely key component of a meadows recovery capacity) with greater potential for replenishment in northern locations and shadows of low replenishment, particularly in the lower portion of north-facing bays (Fig. 5).

The maximum dispersal distance of 'virtual' propagules was 950 km, approximately half the length of the GBR coast line. While this travelled distance may represent a rare event, propagule dispersal over long distances may be critical for adaptability at these scales. Propagules that travel only short distances or remain within the boundary of an existing meadow will have a better chance of remaining in locations likely to be conducive to seagrass growth. However, in the tropics and subtropics, dispersal strategies of marine angiosperms must also operate at scales that explain existing distributions (thousands of kilometres) (Coles *et al.* 2009; McKenzie *et al.* 2010, Waycott *et al.* 2014). Many tropical meadows have persistent viable seed banks but effective methods must be available for longer distance dispersal and replenishment (even if these mechanisms are rare), simply because of the high number of propagules released from meadows over many years. Our modelling demonstrates that most dispersal is limited to short distances, especially when propagules are suspended in the water column, and replenishment is certain to occur within the 30-60 km range. Longer distance dispersal is possible, but likely to be uncommon and have a proportionally reduced role in meadow recovery after loss.

The destructive tropical storms and sediment loads from land runoff from 2007 to 2011 (McKenzie *et al.* 2012; Rasheed *et al.* 2014; McKenna *et al.* 2015) were the catalyst to ask questions regarding propagule dispersal, modes of re-establishment and seagrass recovery in the central GBR. Previous losses of seagrass on the east coast of Queensland have generally recovered naturally in a 3-5 year timeframe (Preen *et al.* 1995; Campbell and McKenzie 2004), but depending on the habitat and location, can take longer (York *et al.* 2014; McKenzie *et al.* 2015), even more than a decade (Birch and Birch 1984). There is little guidance on potential recovery trajectories at the scale of hundreds of kilometres. The results of our study show it would be reasonable to generalise for management in the central GBR that provided there was a healthy meadow nearby and to the south, then re-establishment and/or recovery of a damaged meadow by natural propagule supply would be possible. However, not all meadows have a replenishment potential as great as others (Fig. 5) due to the influences of topography, location and time of year, and individual meadows could be recruitment limited if and when local supplies of propagules are exhausted through disturbance.

Coastal development and watershed impacts from farming and urban and industrial land use have largely been confined to the southern half of the GBR (Grech *et al.* 2011). The results of our study reduce the comfort provided to management by the assumption that the lack of development in the northern GBR provides a buffer to losses in the south. Impacts on meadows from runoff and coastal development in the southern half of the GBR may reduce propagule supply northward, and therefore reduce the replenishment of northern meadows after loss or damage from climatic disturbances. At the scale of the central GBR, southern meadows and meadows in north-facing bays are less likely to be replenished after disturbance events. The lesson from these results more globally is that losses of seagrass meadows may have unexpected consequences for the resilience of meadows many kilometres away. Management actions that protect factors influencing resilience other than dispersal (e.g. genetic diversity, species diversity, energy reserves and seed banks) should target sites with low or potentially low replenishment capacity to improve their post disturbance recovery trajectories. Management actions that protect factors influencing resilience are likely also to lead to enhanced dispersal. Maintaining and enhancing resilient seagrass systems require keeping food webs intact (i.e. balancing herbivore grazing pressure), conserving functionally important species, and ensuring connectivity with adjacent supporting ecosystems (e.g. mangroves; Unsworth *et al.*, 2015).

We have used a “big picture” approach to model the likely interactions among seagrass meadows. This approach has provided valuable insights into how seagrass ecosystems may respond to impacts such as widespread loss after a major storm. These insights can be used to evaluate and improve environmental decision making and marine planning. However, it is important to consider an exercise such as this as a starting point from which to test biological realities and for directing further research in the field to test the parameters that modelling has identified as critical to our understanding.

Acknowledgments

Computational resources were provided by the supercomputing facilities of the Université catholique de Louvain (UCLouvain/CISM) and the Consortium des Équipements de Calcul Intensif en Fédération Wallonie-Bruxelles (CÉCI). Funding for this research was provided by Macquarie University, James Cook University, the Ian Potter Foundation, Sea World Research and Rescue Foundation Inc (SWR/6/15) and Wallonie-Bruxelles International. Many thanks to O. Luiz (Macquarie University) and T. Bridge (Queensland Museum) for assistance with the statistical analysis.

Author contributions

A.G., J.W., C.T., L.M., R.C., M.R., M.W. and E.H. conceived the ideas; A. G., J.W., C.T., E.H., R.C., L.M. and M.R. collected the data; A.G., J.W., E.H. and C.T. analysed the data; and A.G., R.C. and J.W. led the writing, with contributions from all authors.

Biosketch

Alana Grech is a senior lecturer in the Department of Environmental Sciences at Macquarie University. Her research interests focus on modelling the spatial distribution of coastal and marine features, cumulative impact assessment, conservation planning and environmental decision making.

Literature cited

1. Andrews, J.C. & Bode, L. (1988) The tides of the central Great Barrier Reef. *Continental Shelf Research*, 8, 1057-1085.
2. Andrews, J.C. & Furnas, M.J. (1986) Subsurface intrusions of Coral Sea water into the central Great Barrier Reef - I. Structures and shelf-scale dynamics. *Continental Shelf Research*, 6, 491-514.
3. Andutta, F.P., Kingsford, M.J. & Wolanski, E. (2012) 'Sticky water' enables the retention of larvae in a reef mosaic. *Estuarine, Coastal and Shelf Science*, 101, 54-63.
4. Bereuman, M.L., Almany, G.R., Planes, S., Jones, G.P., Saenz-Agudelo, P. & Thorrold, S.R. (2012) Persistence of self-recruitment and patterns of larval connectivity in a marine protected area network. *Ecology and Evolution*, 2(2), 444-452.
5. Berković, B., Cabaco, S., Barrio, J.M., Santos, R., Serrão, E.A. & Alberto, F. (2014) Extending the life history of a clonal aquatic plant: Dispersal potential of sexual and asexual propagules of *Zostera noltii*. *Aquatic Botany,* 113, 123-129.

6. Birch, W. & Birch, M. (1984) Succession and pattern of tropical intertidal seagrasses in Cockle Bay, Queensland, Australia: a decade of observations. *Aquatic Botany*, 19, 343-367.

7. Bode, M., Armsworth, P.R., Fox, H.E. & Bode, L. (2012) Surrogates for reef fish connectivity when designing marine protected area networks. *Marine Ecology Progress Series*, 466, 155-166.

8. Campbell, S.J. & McKenzie, L.J. (2004) Flood related loss and recovery of intertidal seagrass meadows in southern Queensland, Australia. *Estuarine, Coastal and Shelf Science*, 60, 477-490.

9. Carruthers, T., Dennison, W., Longstaff, B., Waycott, M., Abal, E.G., McKenzie, L.J. & Lee Long, W. (2002) Seagrass habitats of north east Australia: models of key processes and controls. *Bulletin of Marine Science*, 71, 1153-1169.

10. Church, J.A. (1987) East Australian current adjacent to the Great Barrier Reef. *Marine and Freshwater Research*, 38, 671-683.

11. Church, J.A. & Boland, F.M. (1983) A permanent undercurrent adjacent to the Great Barrier Reef. *Journal of Physical Oceanography*, 13, 1747-1749.

12. Coles, R.G., Rasheed, M.A., McKenzie, L.J., Grech, A., York, P.H., Sheaves, M., McKenna, S. & Bryant, C. (2015) The Great Barrier Reef World Heritage Area seagrasses: Managing this iconic Australian ecosystem resource for the future. *Estuarine, Coastal and Shelf Science*, 153, A1-A12.

13. Coles, R.G., McKenzie, L.J. & Campbell, S. (2003) The seagrasses of eastern Australia. In: Green, E.P. & Short, F.T. (eds.) *The World Atlas of Seagrasses: Present Status and Future Conservation*. University of California Press, Los Angeles, USA.

14. Coles, R.G., McKenzie, L.J., Dèath, G., Roelofs, A. & Lee Long, W.J. (2009) Spatial distribution of deepwater seagrass in the inter-reef lagoon of the Great Barrier Reef World Heritage Area. *Marine Ecology Progress Series*, 392, 57-68.

15. Coles, R.G., McKenzie, L.J., Rasheed, M.A., Mellors, J., Taylor, H., Dew, K., McKenna, S., Sankey, T., Carter, A. & Grech, A. (2007) *Status and trends of Seagrass Habitats in the Great Barrier Reef World Heritage Area*. Unpublished report to the Marine and Tropical Sciences Research Facility, Reef and Rainforest Research Centre Limited, Cairns, Australia.

16. Egbert, G.D. & Erofeeva, S.Y. (2002) Efficient inverse modeling of Barotropic Ocean tides. *Journal of Atmospheric and Oceanic Technology*, 19 (2), 183-204.

17. Erftemeijer, P., van Beek, J., Ochieng, C., Jager, Z. & Los, H. (2008) Eelgrass seed dispersal via floating generative shoots in the Dutch Wadden Sea: a model approach. *Marine Ecology Progress Series*, 358, 115-124.

18. Geuzaine, C. & Remacle, J.F. (2009) Gmsh: a three-dimensional finite element mesh generator with built-in pre- and post-processing facilities. *International Journal for Numerical Methods in Engineering*, 79(11), 1309-1331.

19. Grech, A. & Coles, R.G. (2010) An ecosystem-scale predictive model of coastal seagrass distribution. *Aquatic Conservation*, 20, 437-444.

20. Grech, A., Coles, R.G. & Marsh, H. (2011) A broad-scale assessment of the risk to coastal seagrasses from cumulative threats. *Marine Policy*, 35, 560-567.

21. Hall, L.M., Hanisak, M.D. & Virnstein, R.W. (2006) Fragments of the seagrasses *Halodule wrightii* and *Halophila johnsonii* as potential recruits in Indian River Lagoon, Florida. *Marine Ecology Progress Series*, 310, 109-117.

22. Hamann, M., Grech, A., Wolanski, E. & Lambrechts, J. (2011) Modelling the fate of marine turtle hatchlings. *Ecological Modelling*, 222, 1515-1521.

23. Harwell, M.C. & Orth, R.J. (2002) Long-distance dispersal potential in a marine macrophyte. *Ecology*, 83, 3319-3330.

24. Hopley, D., Smithers, S.G. & Parnell, K.E. (2007) *The Geomorphology of the Great Barrier Reef: Development, diversity and change.* Cambridge University Press, Cambridge, United Kingdom.

25. Källström, B., Nyqvist, A., Åberg, P., Bodin, M. & André, C. (2008) Seed rafting as a dispersal strategy for eelgrass (*Zostera marina*). *Aquatic Botany*, 88, 148-153.

26. Kendrik, G.A., Waycott, M., Carruthers, T.J.B., Cambridge, M.L., Hovey, R., Krauss, S.L., Lavery, P.S., Les, D.H., Lowe, R.J., Mascaro I Vidal, O., Ooi, J.L.S., Orth, R.J., Rivers, D.O., Ruiz-Montoya, L., Sinclair, E.A., Statton, J., Van Dijk, J.K. & Verduin, J.J. (2012) The central role of dispersal in the maintenance and persistence of seagrass populations. *Bioscience*, 62, 56-65.

27. Kilminster, K., McMahon, K., Waycott, M., Kendrick, G.A., Scanes, P., McKenzie, L.J., O'Brien, K.R., Lyons, M., Ferguson, A., Maxwell, P., Glasby, T. & Udy, J. (2015) Unravelling complexity in seagrass systems for management: Australia as a microcosm. *Science of the Total Environment*, 534, 97-109.

28. Kuo, J. & Kirkman, H. (1992) Fruit, seeds and germination in the seagrass *Halophila ovalis* (Hydrocharitaceae). *Botanica Marina*, 35, 197-204.

29. Kuo, J., Coles, R.G., Lee Long, W.J., & Mellors, J.E. (1991) Fruits and seeds of *Thalassia hemprichii* (Hydrocharitaceae) from Queensland, Australia. *Aquatic Botany*, 40, 165-173.

30. Kuo, J., Lee Long, W.J. & Coles, R.G. (1993) Occurrence and fruit and seed biology of *Halophila tricostata* Greenway (Hydrocharitaceae). *Australian Journal of Marine and Freshwater Research*, 44, 43-57.

31. Lacap, C.D.A., Vermatt, J.E., Rollon, R.N. & Narcoda, H.M. (2002) Propagule dispersal of the SE Asian seagrasses *Enhalus acoroides* and *Thalassia hemprichii. Marine Ecology Progress Series*, 235, 75-80.

32. Lambrechts, J., Hanert, E., Deleersnijder, E., Bernard, P.E., Legat, V., Remacle, J.F. & Wolanski, E. (2008) A multi-scale model of the hydrodynamics of the whole Great Barrier Reef. *Estuarine, Coastal and Shelf Science*, 79, 143-151.

33. Lee Long, W.J, Mellors, J.E. & Coles, R.G. (1993) Seagrasses between Cape York and Hervey Bay, Queensland, Australia. *Australian Journal of Marine and Freshwater Research*, 44, 19-32.

34. LEGRAND, S., DELEERNIJDER, E., HANERT, E., LEGAT, V. & WOLANSKI, E. 2006. High-resolution, unstructured meshes for hydrodynamical models on the Great Barrier Reef (Australia). *Estuarine, Coastal and Shelf Science*, 68, 36-46.

35. Magris, R.A., Pressey, R.L., Weeks, R. & Ban, N.C. (2014) Integrating connectivity and climate change into marine conservation planning. *Biological Conservation*, 170, 207-221.

36. McKenna, S., Jarvis, J., Sankey, T., Reason, C., Coles, R.G. & Rasheed, M. (2015) Declines of seagrasses in a tropical harbour, North Queensland, Australia, are not the result of a single event. *Journal of Biosciences*, 40, 389-398.

37. McKenzie, L.J., Collier, C., Langlois, L., Yoshida, R.L., Smith, N. & Waycott, M. (2015) *Reef Rescue Marine Monitoring Program - Inshore Seagrass, Annual Report for the*

Sampling Period 1st June 2013 – 31st May 2014. Centre for Tropical Water & Aquatic Ecosystem Research (TropWATER), James Cook University, Cairns, Australia.

38. McKenzie, L.J., Collier, C., Waycott, M., Unsworth, R., Yoshida, R.L. & Smith, N. (2012) Monitoring inshore seagrasses of the GBR and responses to water quality. In: Yellowlees, D. & Hughes, T.P. (eds.) *Proceedings of the 12th International Coral Reef Symposium, Cairns, Australia, 9-13 July 2012*. James Cook University, Townsville, Australia.
39. McKenzie, L.J., Yoshida, R.L. & Unsworth, R.K.F. (2014b) Disturbance influences the invasion of a seagrass into an existing meadow. *Marine Pollution Bulletin*, 86, 186-196.
40. McKenzie, L.J., Yoshida, R.L, Grech, A. & Coles, R.G. (2010) *Queensland seagrasses. Status 2010 - Torres Strait and East Coast*. Fisheries Queensland (DEEDI), Cairns, Australia.
41. McKenzie, L.J., Yoshida, R.L., Grech, A. & Coles, R.G. (2014a) Composite of coastal seagrass meadows in Queensland, Australia - November 1984 to June 2010. PANGAEA: http://doi.pangaea.de/10.1594/PANGAEA.826368
42. McMahon, K. (2005) *Recovery of subtropical seagrasses from natural disturbance*. PhD, University of Queensland, Brisbane, Australia.
43. McMahon, K., Van Dijk, K.J, Ruiz-Montoya, L., Kendrick, G.A., Krauss, S.L., Waycott, M., Verduin, J., Lowe, R., Statton, J., Brown, E. & Duarte, C. (2014) The movement ecology of seagrasses. *Proceedings of the Royal Society of London B: Biological Sciences*, 281, 20140878.
44. Nathan, R. & Muller-Landau, H. (2000) Spatial patterns of seed dispersal, their determinants and consequences for recruitment. *Trends in Ecology & Evolution*, 15, 278-285.

45. Nathan, R., Getz, W., Revilla, E., Holyoak, M., Kadmon, R., Saltz, D. & Smouse, P. (2008) A movement ecology paradigm for unifying organismal movement research. *Proceedings of the National Academy of Sciences*, 105, 19052-19059.

46.

47. Oldham, C.E., McMahon, K., Brown, E., Bosserelle, C. & Lavery, P. (2014) A preliminary exploration of the physical properties of seagrass wrack that affect its offshore transport, deposition and retention on a beach. *Limnology & Oceanography: Fluids and Environment.* 4: 120–135.

48. Petus, C., Da Silva, E.T., Devlin, M., Wenger, A.S., & Álvarez-Romero, J. G. (2014) Using MODIS data for mapping of water types within river plumes in the Great Barrier Reef, Australia: Towards the production of river plume risk maps for reef and seagrass ecosystems. *Journal of Environmental Management*, 137, 163-177.

49. Philbrick, C.T. & Les, D.H. (1996) Evolution of aquatic angiosperm reproductive systems. *BioScience*, 46, 813-826.

50. Preen, A.R., Lee Long, W.J. & Coles, R.G. (1995) Flood and cyclone related loss, and partial recovery, of more than 1,000 km2 of seagrass in Hervey Bay, Queensland, Australia. *Aquatic Botany*, 52, 3-17.

51. R Core Team. (2014) *R: A Language and Environment for Statistical Computing*. R Foundation for Statistical Computing, Vienna, Austria.

52. Rasheed, M.A., McKenna, S.A., Carter, A. & Coles, R.G. (2014) Contrasting recovery of shallow and deep-water seagrass communities following climate associated losses in tropical north Queensland, Australia. *Marine Pollution Bulletin*, 83, 491-499.

53. Roberts, C.M., Andelman, S., Branch, G., Bustamante, R.H., Carlos Castilla, J., Dugan, J., Halpern, B.S., Lafferty, K.D., Leslie, H., Lubchenco, J., McCardle, D., Possingham, H.P., Ruckelshaus, M. & Warner, R.R. (2003) Ecological criteria for evaluating candidate sites for marine reserves. *Ecological Applications*, 13, 199-214.

54. Ruiz-Montoya, L., Lowe, R.J. & Kendrick, G.A. (2015) Contemporary connectivity is sustained by wind- and current-driven seed dispersal among seagrass meadows. *Movement Ecology*, 3, 9.

55. Ruiz-Montoya, L., Lowe, R.J., Van Niel, K.P. & Kendrick, G.A. (2015) The role of hydrodynamics on seed dispersal in seagrasses. *Limnology and Oceanography*, 57(5), 1257-1265.

56. Saha, S., Moorthi, S., Wu, X., Wang, J., Nadiga, S., Tripp, P., Behringer, D., Hou, Y.T., Chuang, H.Y., Iredell, M., Ek, M., Meng, H., Yang, R., Mendez, M.P., Van Den Dool, H., Zhang, Q., Wang, W., Chen, M. & Becker, E. (2014) The NCEP Climate Forecast System Version 2. *Journal of Climate*, 27(6), 2185–2208.

57. Spagnol, S., Wolanski, E., Deleersnijder, E., Brinkman, R., McAllister, F., Cushman-Roisin, B. & Hanert, E. (2002) On an error frequently made in the evaluation of advective transport in two-dimensional Lagrangian models of advection-diffusion in coral reef waters. *Marine Ecology Progress Series*, 235, 299-302.

58. Sumoski, S. & Orth, R. (2012) Biotic dispersal in eelgrass Zostera marina. *Marine Ecology Progress Series*, 471, 1-10.

59. Thomas, C.J., Bridge, T.C.L., Figueiredo, J., Deleersnijder, R. & Hanert, E. (2015) Connectivity between submerged and near-sea-surface coral reefs: can submerged reef populations act as refuges? *Diversity and Distributions*, 21(10), 1254-1266.

60. Thomas, C.J., Lambrechts, J., Wolanski, E., Traag, V.A., Blondel, V.D., Deleersnijder, E. & Hanert, E. (2014) Numerical modelling and graph theory tools to study ecological connectivity in the Great Barrier Reef. *Ecological Modelling*, 272, 160-174.

61. Thomson, A.G., York, P., Smith, T., Sherman, C.H., Booth, D., Keough, M., Ross, D.J. & Macreadie, P. (2014) Seagrass viviparous propagules as a potential long-distance dispersal mechanism. *Estuaries and Coasts*, 38, 927-940.

62. Treml, E.A., Halpin, P.N., Urban, D.L. & Pratson, L.F. (2008). Modeling population connectivity by ocean currents, a graph-theoretic approach for marine conservation. *Landscape Ecology*, 23(1), 19-36.

63. Tulipani, D.C. & Lipcius, R.N. (2014) Evidence of eelgrass (*Zostera marina*) seed dispersal by northern diamondback terrapin (*Malaclemys terrapin terrapin*) in lower Chesapeake Bay. *PloS ONE*, 9, e103346.

64. Unsworth, R.K.F., Collier, C.J., Waycott, M., McKenzie, L.J. & Cullen-Unsworth, L.C. (2015) A framework for the resilience of seagrass ecosystems. *Marine Pollution Bulletin*, 100, 34-46.

65. Unsworth, R.K.F., Hinder, S.L., Bodger, O.G. & Cullen-Unsworth, L.C. (2014) Food supply depends on seagrass meadows in the coral triangle. *Environmental Research Letters*, 9, 094005.

66. Waycott, M., McMahon, K.M & Lavery, P. (2014) *A Guide to Southern Temperate Seagrasses.* CSIRO Publishing, Melbourne, Australia.

67. Waycott, M., McMahon, K.M., Mellors, J.E., Calladine, A. & Kleine, D. (2004) *A Guide to Tropical Seagrasses of the Indo-West Pacific*. James Cook University, Townsville, Australia.

68. Weatherall, E.J., Jackson, E.L., Hendry, R.A. & Campbell, M.L. (2016) Quantifying the dispersal potential of seagrass vegetative fragments: A comparison of multiple subtropical species. *Estuarine, Coastal and Shelf Science*. 169, 207-215.

69. Wolanski, E. & Spagnol, S. (2000) Pollution by mud of Great Barrier Reef coastal waters. *Journal of Coastal Research*, 16, 1151-1156.

70. Wolanski, E., Lambrechts, J., Thomas, C.J. & Deleersnijder, E. (2013) The net water circulation through Torres Strait. *Continental Shelf Research*, 64, 66-74.

71. York, P.H., Davies, J.N. & Rasheed, M.A. (2014) *Long-term seagrass monitoring in the Port of Mourilyan – 2013.* Centre for Tropical Water & Aquatic Ecosystem Research (TropWATER) report 14/06, James Cook University, Cairns, Australia.

Tables

Table 1: Date and tide parameters of seagrass dispersal simulations. Two simulations were started at each date to simulate particles that were floating and suspended in the water column.

Simulation	*Start date*	*Tide*
1	August 1	Spring
2	August 5	-
3	August 9	Neap
4	August 13	-
5	August 17	Spring
6	August 20	-
7	August 23	Neap
8	August 26	-
9	August 29	Spring
10	September 3	-
11	September 8	Neap
12	September 11	-
13	September 15	Spring
14	September 18	-
15	September 21	Neap
16	September 23	-
17	September 26	Spring
18	October 1	-
19	October 7	Neap
20	October 10	-
21	October 14	Spring
22	October 17	-
23	October 21	Neap
24	October 24	-
25	October 27	Spring
26	November 2	-
27	November 6	Neap
28	November 10	-
29	November 14	Spring
30	November 17	-
31	November 20	Neap
32	November 22	-
33	November 25	Spring
34	November 28	-

703 **Figure Legends**

704

705 **Figure 1:** (A) Distribution of foundation and non-foundation seagrass meadows in the central
706 Great Barrier Reef; (B) particle release locations off north Hinchinbrook Island; and (C) the
707 location of the central Great Barrier Reef study site relative to Australia.

708

709 **Figure 2:** Discrete habitat units of foundation and non-foundation seagrass meadows in the
710 central Great Barrier Reef. 124 seagrass meadows were grouped into 31 discrete habitat units
711 based on similarities in their seagrass genera and biogeographic properties (i.e. located in the
712 same bay, estuary or island system).

713

714 **Figure 3:** Boxplot of the minimum, first quartile, median, third quartile, and maximum
715 Euclidean (straight line) distance (kilometres) between the release location and the settling
716 location of particles across 34 simulations at each discrete habitat unit (Fig. 2). Data in the top
717 graph did not include a wind advection coefficient and simulated seagrass propagules suspended
718 in the water column; data in the bottom graph included a 2% wind advection coefficient to
719 simulate the dispersal of floating seagrass propagules.

720

721 **Fig. 4:** Wind roses of the proportion (%) of particles dispersed at various directions and distances
722 from their origin of simulations that were: (A) floating; and (B) suspended in the water column.

723

724 **Fig. 5:** Potential replenishment index for foundation and non-foundation species when particles
725 float (E and F respectively), are suspended (C and D) in the water column, and both floating and

suspended (combined; A and B). Particle supply was mapped by multiplying the logarithm of the number of settled 'virtual' propagules by the number of source discrete habitat units at each grid cell.

730 **Figure 1:** (A) Distribution of foundation and non-foundation seagrass meadows in the central
731 Great Barrier Reef; (B) particle release locations off north Hinchinbrook Island; and (C) the
732 location of the central Great Barrier Reef study site relative to Australia.
733

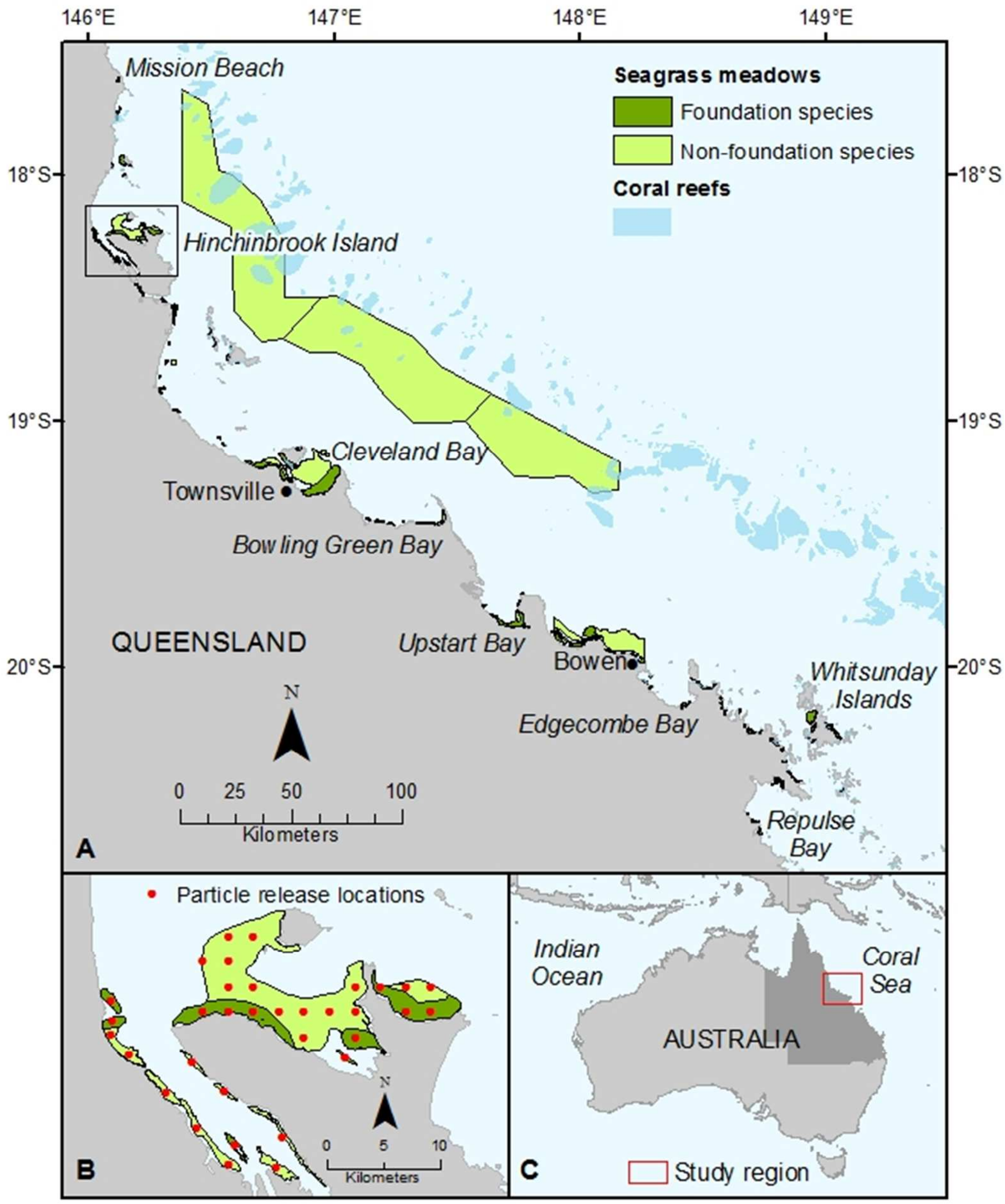

734

Figure 2: Discrete habitat units of foundation and non-foundation seagrass meadows in the central Great Barrier Reef. 124 seagrass meadows were grouped into 31 discrete habitat units based on similarities in their seagrass genera and biogeographic properties (i.e. located in the same bay, estuary or island system).

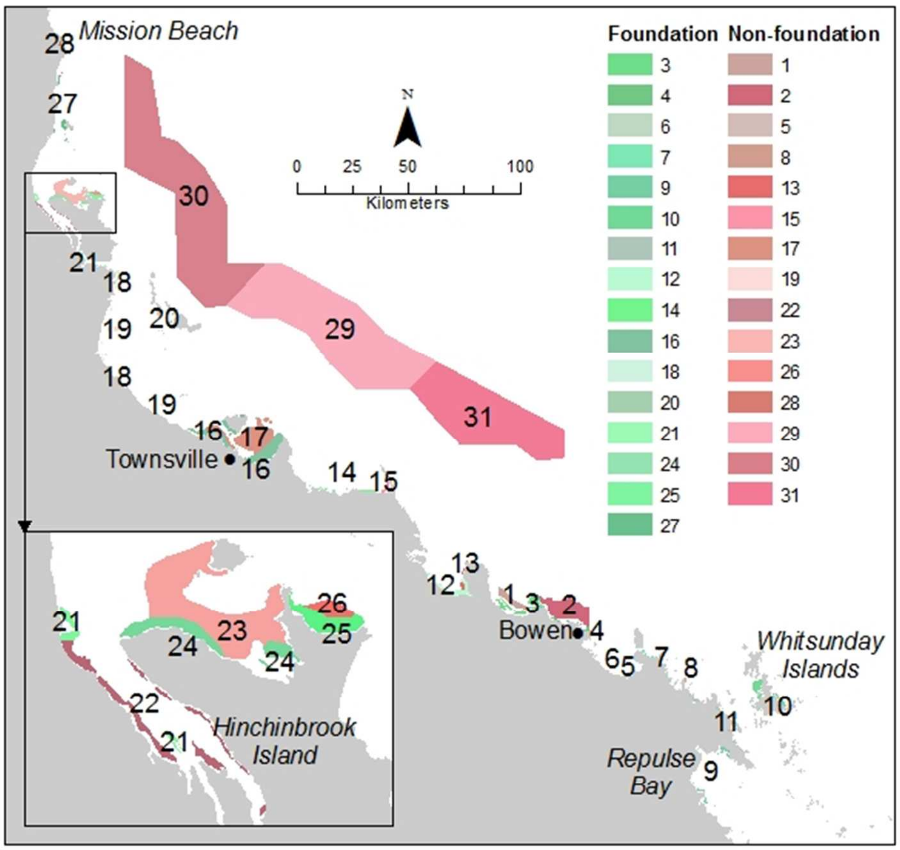

Figure 3: Boxplot of the minimum, first quartile, median, third quartile, and maximum Euclidean (straight line) distance (kilometres) between the release location and the settling location of particles across 34 simulations at each discrete habitat unit (Fig. 2). Data in the top graph did not include a wind advection coefficient and simulated seagrass propagules suspended in the water column; data in the bottom graph included a 2% wind advection coefficient to simulate the dispersal of floating seagrass propagules.

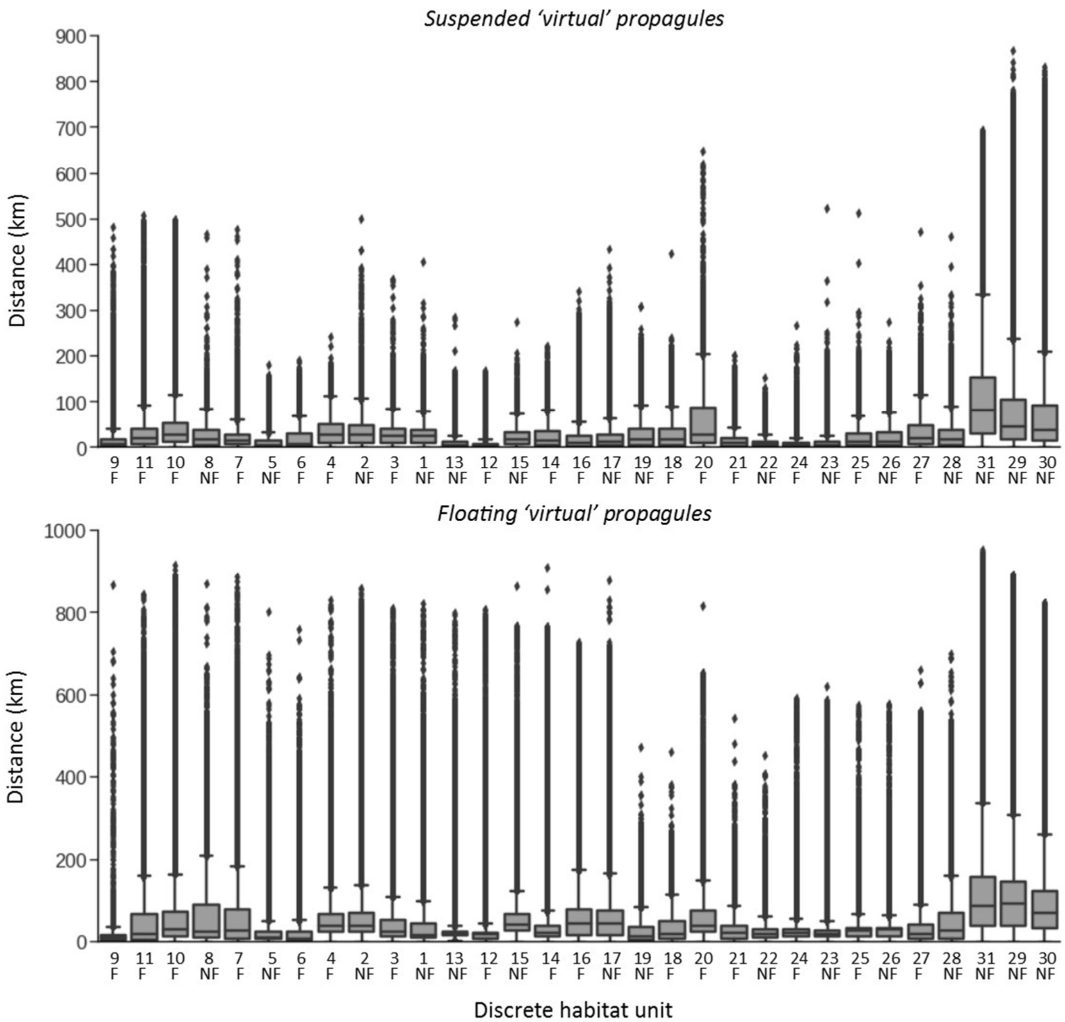

749 **Fig. 4:** Wind roses of the proportion (%) of particles dispersed at various directions and distances
750 from their origin of simulations that were: (A) floating; and (B) suspended in the water column.
751

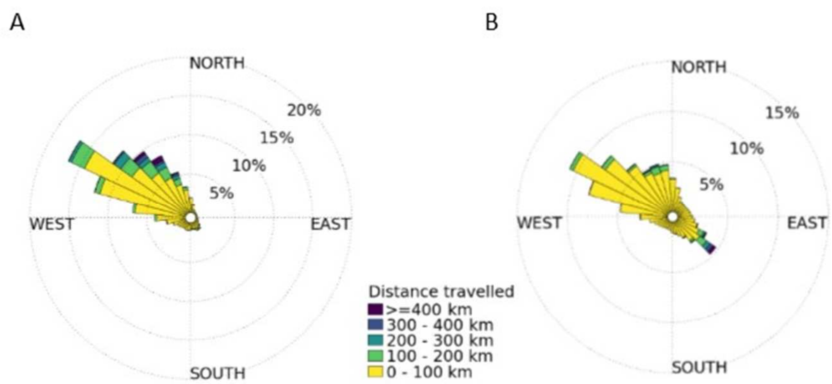

752
753

Fig. 5: Potential replenishment index for foundation and non-foundation species when particles float (E and F respectively), are suspended (C and D) in the water column, and both floating and suspended (combined; A and B). Particle supply was mapped by multiplying the logarithm of the number of settled ‘virtual’ propagules by the number of source discrete habitat units at each grid cell.

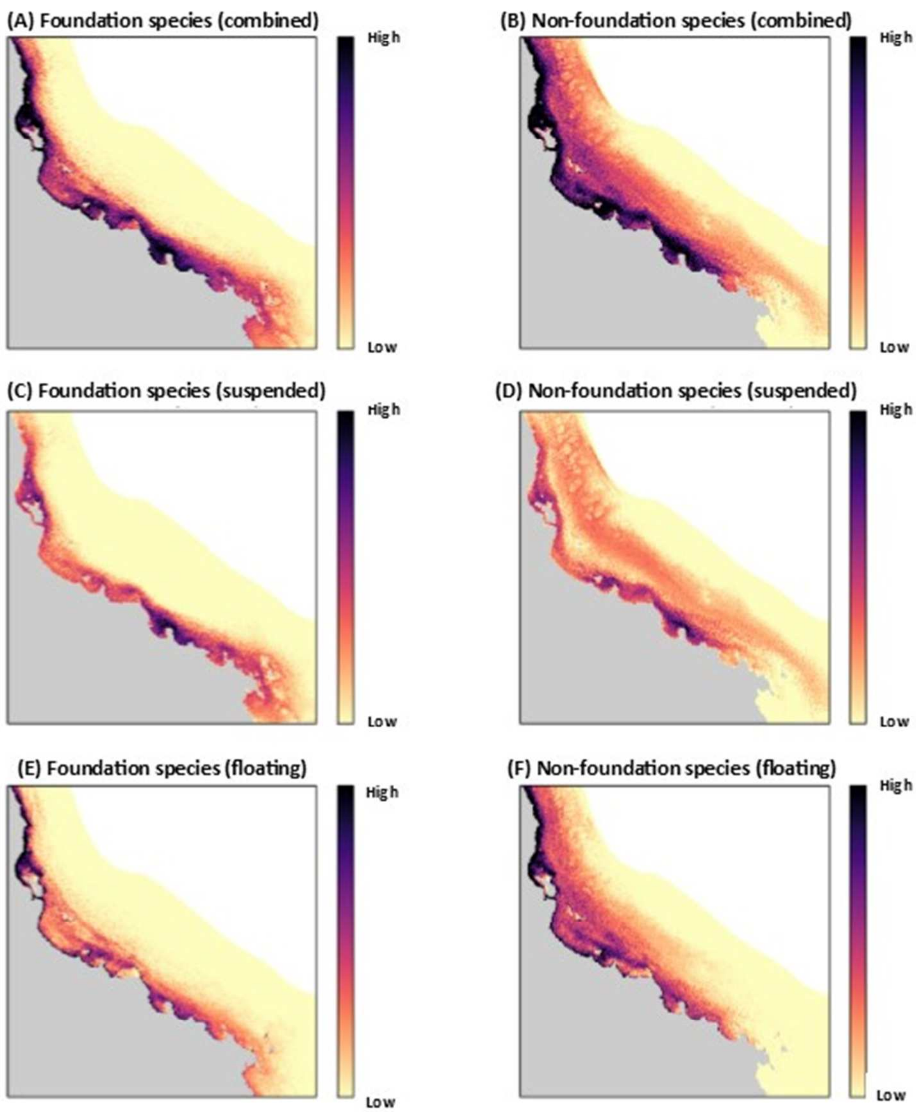

761 **Supporting Information**

762 Additional Supporting Information may be found in the online version of this article:

763 **Table S1:** Attributes of 124 seagrass meadows.

764 **Fig. S1:** Graph of the first-order decay function.

765 **Appendix S1:** Animations of the dispersal of particles representing ‘virtual’ seagrass propagules.

766 **Table S2:** Results of the linear mixed-effect model.

767

Table S1: Attributes of 124 seagrass meadows. Deep-water seagrass habitats are meadows 122, 123 and 124.

Meadow ID	*Discrete habitat unit ID*	*Species class*	*Number of release locations*	*Area km^2*
1	9	Foundation	1	3.07
2	9	Foundation	1	3.14
3	9	Foundation	1	0.50
4	10	Foundation	1	0.42
5	9	Foundation	1	0.75
6	9	Foundation	3	8.35
7	11	Foundation	1	2.75
8	11	Foundation	1	0.71
9	11	Foundation	1	0.74
10	11	Foundation	1	1.76
11	10	Foundation	1	0.67
12	11	Foundation	1	2.05
13	10	Foundation	1	0.55
14	11	Foundation	1	0.64
15	10	Foundation	2	3.63
16	11	Foundation	1	4.56
17	10	Foundation	1	0.80
18	11	Foundation	1	0.61
19	10	Foundation	1	2.45
20	10	Foundation	1	4.06
21	10	Foundation	1	0.51
22	7	Foundation	1	0.81
23	10	Foundation	4	17.86
24	8	Non-foundation	1	0.64
25	7	Foundation	1	0.43
26	6	Foundation	1	3.54
27	7	Foundation	1	1.05
28	5	Non-foundation	1	0.52
29	7	Foundation	1	0.49
30	7	Foundation	1	1.41
31	7	Foundation	1	0.55
32	5	Non-foundation	1	0.73
33	7	Foundation	1	0.55
34	7	Foundation	1	1.60
35	6	Foundation	1	2.36

36	7	Foundation	1	0.52
37	6	Foundation	1	0.50
38	4	Foundation	1	3.57
39	4	Foundation	1	0.54
40	4	Foundation	1	0.97
41	4	Foundation	1	1.22
42	4	Foundation	1	1.09
43	3	Foundation	1	0.68
44	3	Foundation	1	0.89
45	3	Foundation	3	7.84
46	3	Foundation	1	2.47
47	3	Foundation	1	2.34
48	3	Foundation	3	13.00
49	2	Non-foundation	35	155.00
50	1	Non-foundation	7	38.18
51	12	Foundation	7	30.11
52	12	Foundation	1	1.37
53	13	Non-foundation	1	1.04
54	13	Non-foundation	1	0.42
55	14	Foundation	1	0.44
56	14	Foundation	1	0.75
57	14	Foundation	2	4.04
58	14	Foundation	1	0.42
59	14	Foundation	1	0.51
60	14	Foundation	1	0.82
61	14	Foundation	1	0.90
62	15	Non-foundation	2	7.85
63	17	Non-foundation	1	0.99
64	16	Foundation	6	28.36
65	17	Non-foundation	1	1.18
66	16	Foundation	3	12.17
67	17	Non-foundation	1	3.86
68	17	Non-foundation	32	145.58
69	16	Foundation	1	0.81
70	17	Non-foundation	1	0.66
71	19	Non-foundation	1	1.12
72	19	Non-foundation	1	1.20
73	19	Non-foundation	1	0.73
74	18	Foundation	1	0.94
75	18	Foundation	1	0.81
76	19	Non-foundation	1	0.58
77	19	Non-foundation	1	0.70
78	19	Non-foundation	1	0.65

79	20	Foundation	1	1.01
80	19	Non-foundation	1	1.82
81	19	Non-foundation	1	3.74
82	20	Foundation	1	1.88
83	20	Foundation	1	0.45
84	19	Non-foundation	1	0.72
85	20	Foundation	1	1.44
86	20	Foundation	1	0.66
87	18	Foundation	1	2.77
88	18	Foundation	1	1.00
89	18	Foundation	1	1.80
90	18	Foundation	1	2.24
91	21	Foundation	1	2.24
92	21	Foundation	1	0.81
93	21	Foundation	1	0.59
94	21	Foundation	1	0.50
95	22	Non-foundation	1	0.41
96	22	Non-foundation	1	2.60
97	21	Foundation	1	1.01
98	22	Non-foundation	1	2.22
99	22	Non-foundation	1	0.61
100	22	Non-foundation	3	6.39
101	22	Non-foundation	1	0.75
102	24	Foundation	1	0.48
103	22	Non-foundation	2	3.64
104	21	Foundation	1	1.66
105	25	Foundation	3	11.41
106	23	Non-foundation	12	68.35
107	27	Foundation	1	0.47
108	27	Foundation	1	0.62
109	27	Foundation	2	7.67
110	27	Foundation	1	2.27
111	28	Non-foundation	1	0.51
112	28	Non-foundation	1	0.53
113	28	Non-foundation	1	1.43
114	16	Foundation	21	88.30
115	17	Non-foundation	6	23.68
116	13	Non-foundation	1	5.34
117	3	Foundation	3	18.24
118	21	Foundation	1	1.52
119	24	Foundation	3	11.55
120	24	Foundation	1	4.44
121	26	Non-foundation	2	5.37

122	29	Non-foundation	18	2083.13
123	30	Non-foundation	23	2314.63
124	31	Non-foundation	12	1394.75

Fig. S1: Graph of the first-order decay function used to simulate the gradual settlement of particles over the eight week modelling period (Erftemeijer *et al.* 2008).

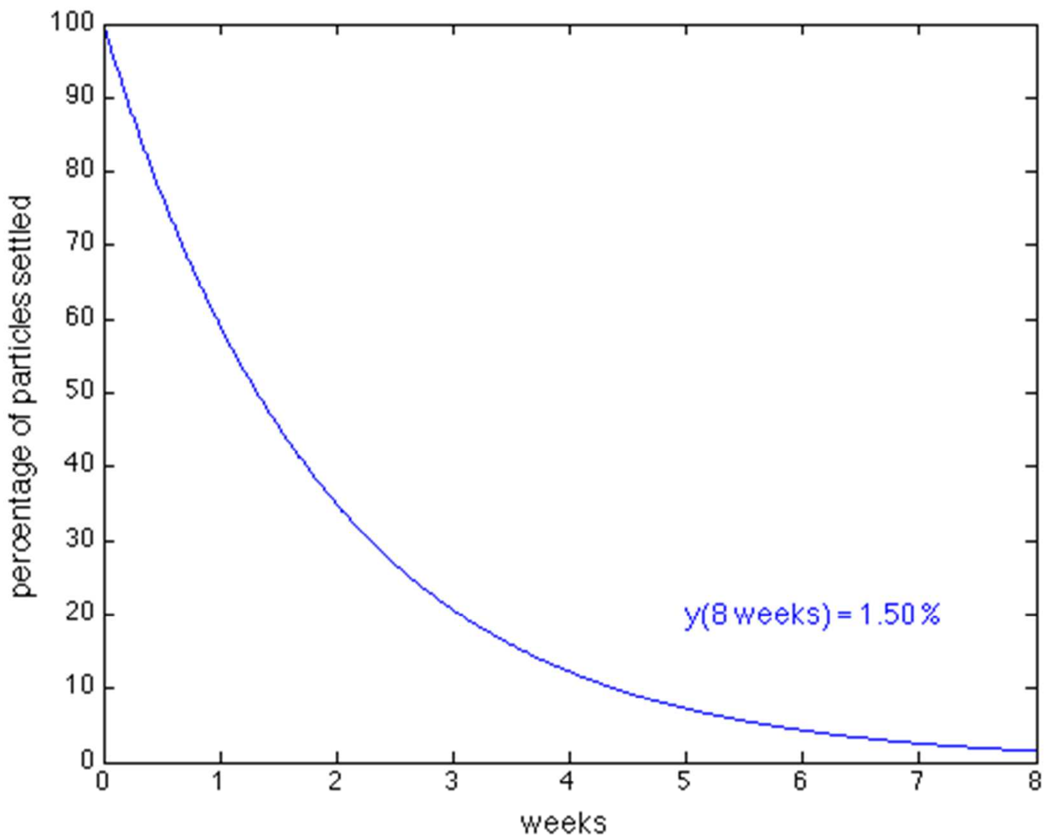

Appendix S1: Animations showing the dispersal of particles for discrete habitat units 3, 16, 24 and 29 (Fig. 2) at four start dates. Only those particles still in movement are displayed (i.e. settled particles are not displayed).

Discrete habitat unit ID	*Species class*	*Fraction*	*Start date*	*File name*
3	Foundation	Suspended	1 August	0801N3_sub
3	Foundation	Floating	1 August	0801N3_sur
16	Foundation	Suspended	1 August	0801N16_sub
16	Foundation	Floating	1 August	0801N16_sur
24	Non-foundation	Suspended	1 August	0801N24_sub
24	Non-foundation	Floating	1 August	0801N24_sur
29	Non-foundation	Suspended	1 August	0801N29_sub
29	Non-foundation	Floating	1 August	0801N29_sur
3	Foundation	Suspended	3 September	0903N3_sub
3	Foundation	Floating	3 September	0903N3_sur
16	Foundation	Suspended	3 September	0903N16_sub
16	Foundation	Floating	3 September	0903N16_sur
24	Non-foundation	Suspended	3 September	0903N24_sub
24	Non-foundation	Floating	3 September	0903N24_sur
29	Non-foundation	Suspended	3 September	0903N29_sub
29	Non-foundation	Floating	3 September	0903N29_sur
3	Foundation	Suspended	1 October	1001N3_sub
3	Foundation	Floating	1 October	1001N3_sur
16	Foundation	Suspended	1 October	1001N16_sub
16	Foundation	Floating	1 October	1001N16_sur
24	Non-foundation	Suspended	1 October	1001N24_sub
24	Non-foundation	Floating	1 October	1001N24_sur
29	Non-foundation	Suspended	1 October	1001N29_sub
29	Non-foundation	Floating	1 October	1001N29_sur
3	Foundation	Suspended	2 November	1102N3_sub
3	Foundation	Floating	2 November	1102N3_sur
16	Foundation	Suspended	2 November	1102N16_sub
16	Foundation	Floating	2 November	1102N16_sur
24	Non-foundation	Suspended	2 November	1102N24_sub
24	Non-foundation	Floating	2 November	1102N24_sur
29	Non-foundation	Suspended	2 November	1102N29_sub
29	Non-foundation	Floating	2 November	1102N29_sur

Table S2: Results of linear mixed-effect model to test for to significant effects of predictor variables on the dispersal distance (*distance*) at each release location of (A) floating 'virtual' propagules and (B) suspended 'virtual' propagules: month of release (*month*); tide on start date of simulation (*tide*); depth (*depth*); species (*species*); and distance to coast (*coast*). Dispersal distance was aggregated at each release location for the 34 simulations of floating propagules and the 34 simulations of suspended propagules, and the 95th percentile calculated.

(A) Floating 'virtual' propagules

Summary statistics full model

	Value	Std.Error	DF	t-value	p-value
(Intercept)	5.453471	0.19474034	10522	28.00381	<0.001
Fmonth November	-1.476736	0.01355755	10522	-108.92351	<0.001
Fmonth October	-1.43034	0.01393982	10522	-102.60823	<0.001
Fmonth September	-1.372027	0.01393982	10522	-98.425	<0.001
Fspecies Non-foundation	-0.023565	0.05629774	315	-0.41858	0.6758
Ftide Neap	-0.001098	0.0122822	10522	-0.08936	0.9288
Ftide Spring	-0.062758	0.01185855	10522	-5.29225	<0.001
Fdepth Intertidal/Subtidal	-0.70966	0.08384329	315	-8.46412	<0.001
log(coast + 1)	0.089379	0.01838781	315	4.86075	<0.001

Model selection table

Global model call: lme.formula(fixed = log(distance) ~ fmonth + fspecies + ftide + fdepth + log(coast + 1) data = floating random = ~1 | frelease location)

(Int)	fdp	fmn	fsp	ftd	log(coast+1)	df	logLik	AICc	deltaAIC	weight
28 5.459	+	+		+	0.08669	10	-8641.124	17302.3	0	0.945

32	5.453	+	+	+	+	0.08938	11	-8642.995	17308	5.75	0.053
20	5.438	+	+			0.08669	8	-8649.633	17315.3	13.01	0.001
12	6.389	+	+		+		9	-8650.222	17318.5	16.19	0
24	5.432	+	+	+		0.08938	9	-8651.504	17321	18.76	0

788

Final Model

	Value	Std.Error	DF	t-value	p-value
(Intercept)	5.458697	0.19408655	10522	28.12507	<0.001
Fmonth November	-1.476736	0.01355755	10522	-108.92351	<0.001
Fmonth October	-1.43034	0.01393982	10522	-102.60823	<0.001
Fmonth September	-1.372027	0.01393982	10522	-98.425	<0.001
Ftide Neap	-0.001098	0.0122822	10522	-0.08936	0.9288
Ftide Spring	-0.062758	0.01185855	10522	-5.29225	<0.001
Fdepth Intertidal/Subtidal	-0.705696	0.08319806	316	-8.48213	<0.001
log(coast + 1)	0.086695	0.01721124	316	5.03711	<0.001

789

790 (B) Suspended ‘virtual’ propagules

791

Summary statistics full model

	Value	Std.Error	DF	t-value	p-value
(Intercept)	4.305612	0.21428961	10522	20.09249	<0.001
Fmonth November	-0.058105	0.01109378	10522	-5.237635	<0.001
Fmonth October	0.170247	0.01140658	10522	14.925327	<0.001
Fmonth September	0.063067	0.01140658	10522	5.528976	<0.001
Fspecie Non-foundation	-0.217867	0.06198484	315	-3.514842	<0.001
Ftide Neap	-0.004428	0.0100502	10522	-0.440563	0.6595
Ftide Spring	0.00615	0.00970353	10522	0.633784	0.5262
Fdepth Intertidal/Subtidal	-1.045538	0.09231299	315	-11.326008	<0.001
log(coast + 1)	0.105338	0.02024531	315	5.203069	<0.001

792

Model selection table

Global model call: lme.formula(fixed = log(distance) ~ fmonth + fspecies + ftide + fdepth + log(coast + 1) data = suspended random = ~1 | frelease location)

(Int)	fdp	fmn	fsp	ftd	log(coast+1)	df	logLik	AICc	deltaAIC	weight
4.307	+	+	+		0.1053	9	-6556.011	13130	0	0.961
4.355	+	+			0.08053	8	-6560.227	13136.5	6.43	0.039
5.219	+	+				7	-6565.687	13145.4	15.34	0
4.306	+	+	+	+	0.1053	11	-6563.028	13148.1	18.04	0
5.324	+	+	+			8	-6566.056	13148.1	18.09	0

Final Model

	Value	Std.Error	DF	t-value	p-value
(Intercept)	4.306678	0.2142423	10524	20.101903	<0.001
Fmonth November	-0.058788	0.01104067	10524	-5.324719	<0.001
Fmonth October	0.169611	0.01138047	10524	14.903732	<0.001
Fmonth September	0.062431	0.01138047	10524	5.485821	<0.001
Fspecie Non-foundation	-0.217867	0.06198484	315	-3.514842	<0.001
Fdepth Intertidal/Subtidal	-1.045538	0.09231299	315	-11.326008	<0.001
log(coast + 1)	0.105338	0.02024531	315	5.203069	<0.001

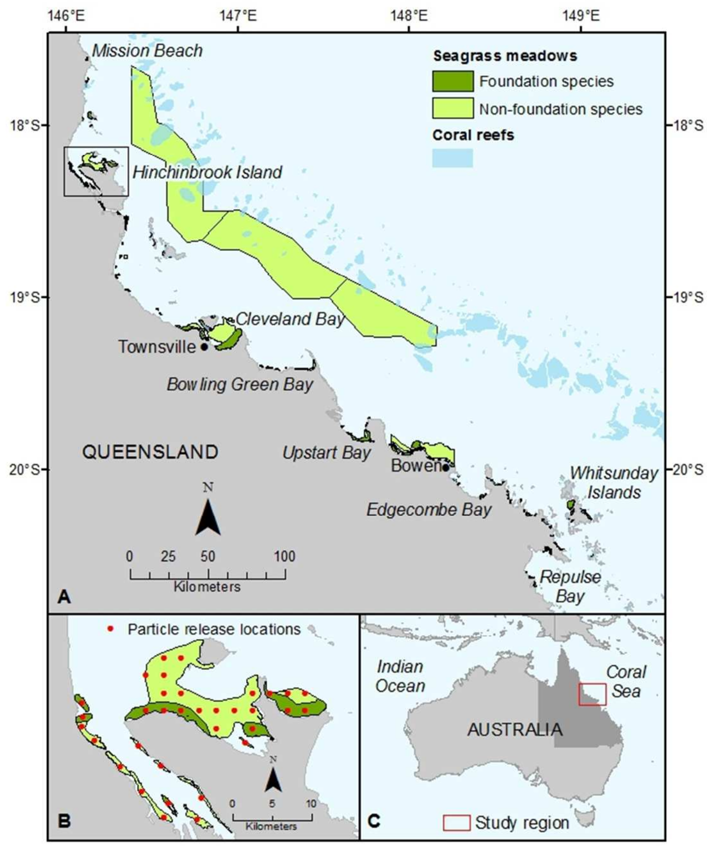

(A) Distribution of foundation and non-foundation seagrass meadows in the central Great Barrier Reef; (B) particle release locations off north Hinchinbrook Island; and (C) the location of the central Great Barrier Reef study site relative to Australia.

Fig. 1

210x296mm (96 x 96 DPI)

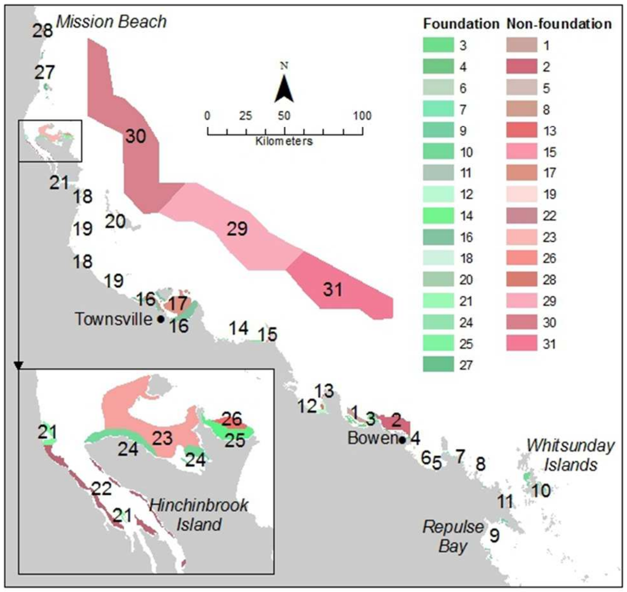

Discrete habitat units of foundation and non-foundation seagrass meadows in the central Great Barrier Reef. 124 seagrass meadows were grouped into 31 discrete habitat units based on similarities in their seagrass genera and biogeographic properties (i.e. located in the same bay, estuary or island system).
Fig. 2
210x296mm (96 x 96 DPI)

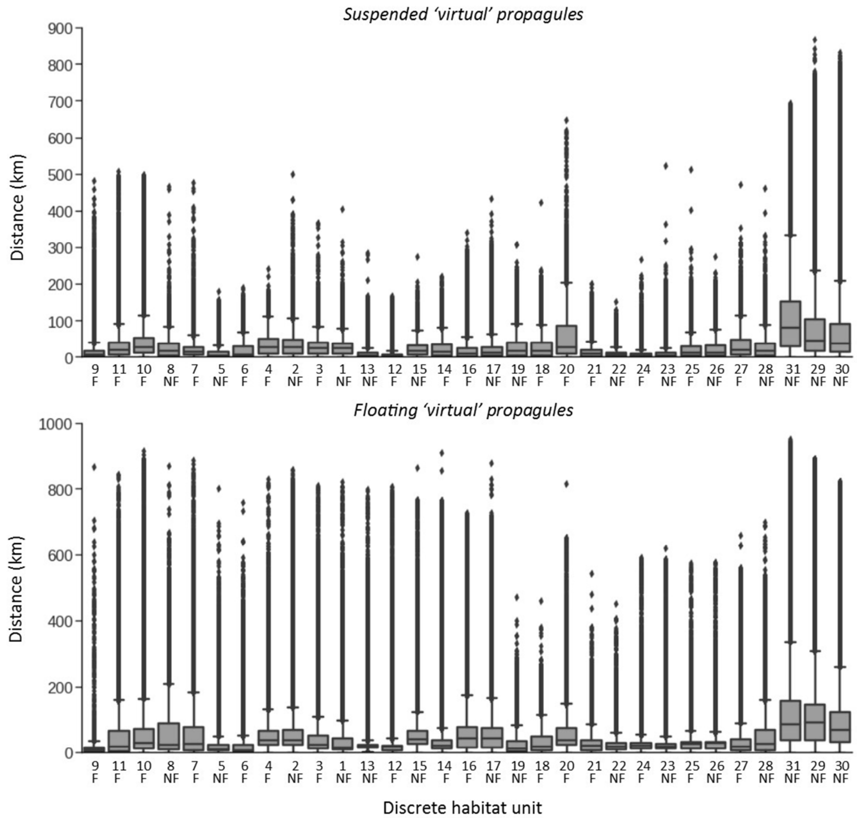

Boxplot of the minimum, first quartile, median, third quartile, and maximum Euclidean (straight line) distance (kilometres) between the release location and the settling location of particles across 34 simulations at each discrete habitat unit (Fig. 2). Data in the top graph did not include a wind advection coefficient and simulated seagrass propagules suspended in the water column; data in the bottom graph included a 2% wind advection coefficient to simulate the dispersal of floating seagrass propagules.

Fig. 3

219x199mm (150 x 150 DPI)

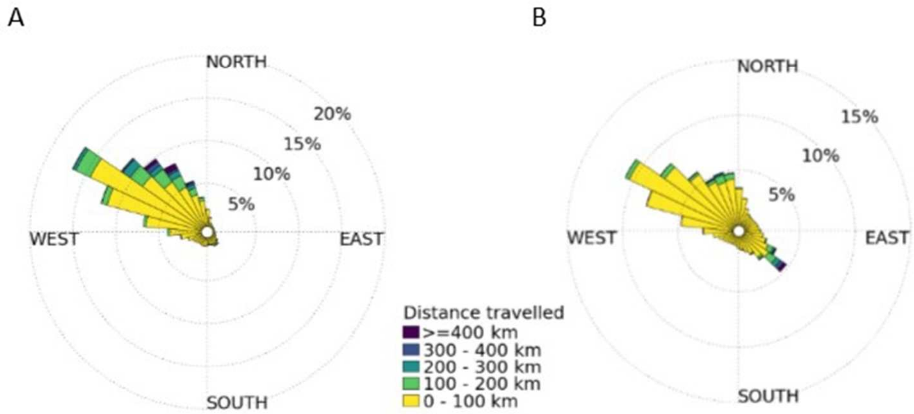

Wind roses of the proportion (%) of particles dispersed at various directions and distances from their origin of simulations that were: (A) floating; and (B) suspended in the water column.

Fig. 4

120x59mm (150 x 150 DPI)

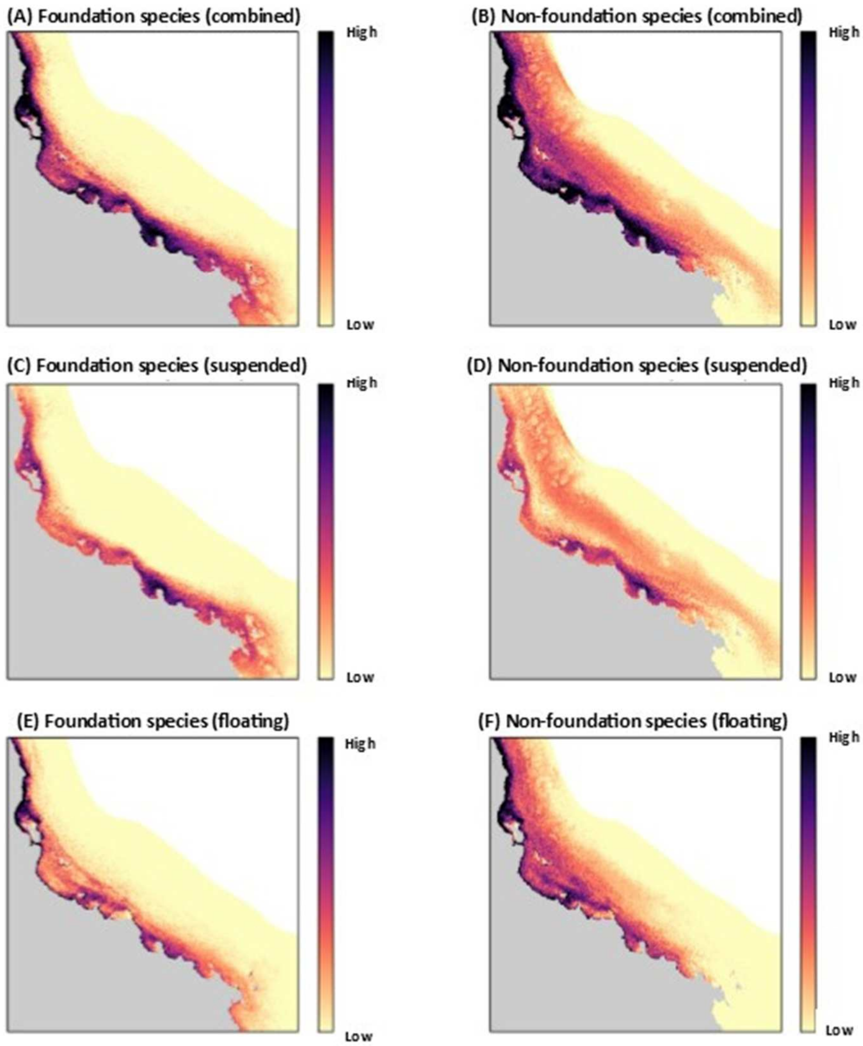

Potential replenishment index for foundation and non-foundation species when particles float (E and F respectively), are suspended (C and D) in the water column, and both floating and suspended (combined; A and B). Particle supply was mapped by multiplying the logarithm of the number of settled 'virtual' propagules by the number of source discrete habitat units at each grid cell.

Fig. 5

99x124mm (150 x 150 DPI)